Large tunneling magnetoresistance in GaMnAs/AlAs/GaMnAs ferromagnetic semiconductor tunnel junctions

Masaaki Tanaka* and Yutaka Higo
Department of Electronic Engineering, University of Tokyo

We have observed very large tunneling magnetoresistance (TMR) in epitaxially grown $Ga_{1-x}Mn_x$-As/AlAs/$Ga_{1-x}Mn_x$As ferromagnetic semiconductor tunnel junctions. Large TMR ratios more than 70% were obtained in junctions with a very thin ($\leqq$ 1.6 nm) AlAs tunnel barrier when the magnetic field was applied along the [100] axis in the film plane. The TMR was found to rapidly decrease with increasing the barrier thickness, which is explained by calculations assuming that the parallel wavevector of carriers is conserved in tunneling.

In the past few years, tunneling magnetoresistance (TMR) and related phenomena were extensively studied in magnetic tunnel junctions (MTJs),[1,2] leading to important applications such as magnetic field sensors and magnetic random access memory (MRAM).[3,4] In most of the experiments on spin-polarized tunneling in ferromagnet (FM) / insulator (I) / ferromagnet (FM) tunnel junctions, polycrystalline transition metals and amorphous oxides are used as FM and I layers, respectively.

On the other hand, ferromagnetic semiconductor heterostructures based on $Ga_{1-x}Mn_x$As can give a new interesting opportunity to study spin-dependent transport phenomena. Because $Ga_{1-x}Mn_x$As is a ferromagnetic p-type semiconductor with the zincblende type crystal structure having almost the same lattice constant as GaAs and AlAs, $Ga_{1-x}Mn_x$As/ (GaAs or AlAs) III-V based heterostructures can be epitaxially grown with abrupt interfaces and with atomically controlled layer thickness.[5–8] Although the Curie temperature of $Ga_{1-x}Mn_x$As is below room temperature so far (at most 110 K [7]), using GaMnAs based III-V heterostructures as tunnel junctions would have several advantages: (1) One can form high-quality single-crystalline MTJs made of all-semiconductor heterostructures, which can be easily integrated with other III-V based structures and devices. (2) In principle, many parameters such as the barrier height, the barrier thickness, and the Fermi energy of FM electrodes are controllable. (3) Introduction of quantum heterostructures such as double-barrier resonant tunneling diodes is easier than any other material system.[9] At this moment, however, little is understood on the spin polarized tunneling in such ferromagnetic semiconductor heterostructure system.

We have recently observed TMR in a $Ga_{1-x}Mn_x$As/AlAs/ $Ga_{1-x}Mn_x$As tunnel junction with the magnetic field applied in plane along the [110] direction.[10] Although the total change in the tunnel resistance $\Delta R/R$ measured at 4.2 K was 44% including the slowly saturating negative component at higher magnetic field, the TMR ratio purely due to the spin-valve effect was estimated to be only 15–19% in our previous paper.[10] More recently, Chiba *et al.*[11] also reported a TMR ratio of 5.5% at 20 K in a $Ga_{1-x}Mn_x$As tunnel junction.

* e-mail address: masaaki@ee.t.u-tokyo.ac.jp

In this letter, we report on by far larger TMR ratios (> 70%) at 8 K in $Ga_{1-x}Mn_x$As/AlAs/$Ga_{1-x}Mn_x$As tunnel junctions, which is purely due to the change of the magnetization direction of the two electrodes. We have studied the dependence of the TMR on the barrier thickness in a wedge-type sample, and have found that the TMR ratio rapidly decreases with increasing the barrier thickness d_{AlAs} in junctions with $d_{\mathrm{AlAs}} > 1.5$ nm. This barrier thickness dependence of the TMR can be explained by tight-binding calculations of tunneling assuming that the wavevector in the direction parallel to the interface is conserved.

Figure 1 (a) illustrates the sample structure prepared by low temperature molecular beam epitaxy (LT-MBE). After a 100 nm-thick Be-doped GaAs buffer layer was grown at 580°C on a p^+-GaAs (001) substrate, a $Ga_{1-x}Mn_x$As ($x =$ 4.0%, 50 nm)/ AlAs(d_{AlAs})/ $Ga_{1-x}Mn_x$As ($x = 3.3\%$, 50 nm) trilayer was grown at 250°C. By using a shutter linearly moving in front of the substrate, we changed the barrier thickness d_{AlAs} ranging from 1.3 nm to 2.8 nm within a wafer of $20 \times 20\,\mathrm{mm}^2$. The slope of the wedge was estimated by the growth rate of AlAs, which was obtained by reflection high energy electron diffraction (RHEED) oscillations, and the moving speed of the shutter. Preparation of wedge-type samples is important in order to measure the dependence of the TMR of MTJs on the barrier thickness, because the electronic and magnetic properties of the GaMnAs layers are very sensitive to the growth conditions.[12] In addition, undoped 1 nm-thick GaAs spacers were inserted between GaMnAs and AlAs to avoid Mn diffusion into the barrier, which causes spin-flip scattering, and to make the interfaces smooth. In order to measure tunneling transport, the sample was patterned by photolithography and mesa etching into arrays of round-shaped junctions with 200 μm in diameter with various barrier thicknesses ranging from 1.3 nm to 2.8 nm.

The magnetization of the $Ga_{1-x}Mn_x$As ($x = 4.0\%$, 50 nm)/ AlAs (3 nm)/ $Ga_{1-x}Mn_x$As ($x = 3.3\%$, 50 nm) trilayer measured by SQUID at 8 K is shown in Fig. 1 (b). In the SQUID measurements, the trilayer sample was cleaved into a square shape with the area of $3 \times 3\,\mathrm{mm}^2$. The magnetic field was applied along the [100] axis in the plane. Pairs of arrows in the figure indicate the configuration of the two magnetiza-

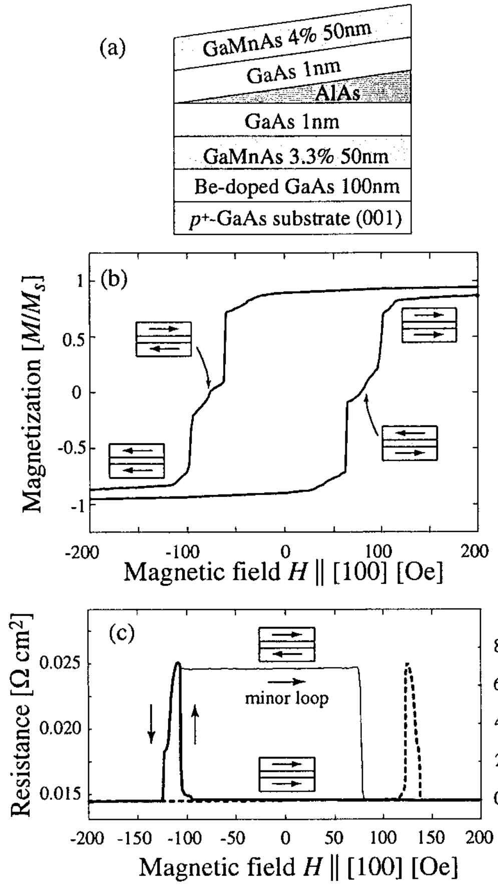

Fig. 1. (a) Schematic illustration of a wedge-type ferromagnetic semiconductor trilayer heterostructure sample grown by LT-MBE. (b) Magnetization of a $Ga_{1-x}Mn_xAs$(x = 4.0%, 50 nm)/ AlAs(3 nm)/ $Ga_{1-x}Mn_xAs$(x = 3.3%, 50 nm) trilayer measured by SQUID at 8 K. The specimen size was $3\times3\,\mathrm{mm}^2$. The vertical axis shows the normalized magnetization M/M_s, where M_s is the saturation magnetization. (c) TMR curves at 8 K of a Magnetization of a $Ga_{1-x}Mn_xAs$(x = 4.0%, 50 nm)/ AlAs(1.6 nm)/ $Ga_{1-x}Mn_xAs$(x = 3.3%, 50 nm) tunnel junction. The tunnel junctions were mesa-etched round-shaped diodes with 200 μm in diameter. Bold solid and dashed curves are major loops, with the magnetic field sweep direction from positive to negative and negative to positive, respectively. A minor loop is shown by a thin solid curve. In both (b) and (c), the magnetic field was applied along the [100] axis in the plane.

tions at different fields. Due to the different coercivity of the two GaMnAs layers, we observed a double-step magnetization curve with coercive fields of about 60 Oe and 100 Oe.

Figure 1 (c) shows tunnel resistance vs. magnetic field, that is, TMR curves measured at 8 K on a junction with $d_{\mathrm{AlAs}} = 1.6$ nm when the magnetic field was applied along the [100] axis in the plane. The TMR is defined here as $(R(H) - R(0))/R(H)$, where $R(H)$ is the resistance at the field of H. Bold solid and dashed curves were obtained by sweeping the field from positive to negative and negative to positive, respectively. As shown by the bold solid curve, when the field was swept from the positive saturation field down to negative, the TMR suddenly increased at $H = -110$ Oe when the magnetization of one GaMnAs layer reversed and the configuration of the two magnetizations changed from parallel to antiparallel. Then, sweeping the field further to the negative direction, the TMR decreased to the initial value at $H = -125$ Oe when the magnetization of the other GaMnAs layer reversed and the configuration of the two magnetizations became parallel again. The difference of the coercive fields between the M–H curve in Fig. 1 (b) and the TMR curve in Fig. 1 (c) is caused by the difference of the shape and size of the measured samples. Note that the TMR value is over 70%, much higher than the previous reports.[10,11] As shown by a thin solid curve in Fig. 1 (c), when we measured a minor loop by reversing the sweep direction of the field at the antiparallel configuration at $H = -110$ Oe, the TMR in the antiparallel configuration was kept until the magnetization first reversed was reversed again and the TMR suddenly dropped at $H = 70$ Oe. This fact shows that the antiparallel configuration is stable as well as the parallel configuration.

Figure 2 (a) shows the tunnel resistance R for the tunnel junctions measured at 8 K as a function of the barrier thickness d_{AlAs}. The resistance exponentially increased from $10^{-3}\,\Omega\mathrm{cm}^2$ to $10\,\Omega\mathrm{cm}^2$ as d_{AlAs} increased, which means that high-quality tunnel junctions were formed with a constant barrier height. In the WKB approximation, the slope of $\ln R - d_{\mathrm{AlAs}}$ characteristics is given by $2[2m^*V_b]^{1/2}\hbar$, thereby the product m^*V_b is estimated to be $0.32m_0$ [kg·eV], where m_0 is the free-electron mass, m^* is the effective mass of holes, and V_b is the barrier height.[13]

Figure 2 (b) shows barrier thickness dependence of TMR at 8 K when the magnetic field was applied in-plane along the [100] and [$1\bar{1}0$] axes. The maximum TMR was 75% at $d_{\mathrm{AlAs}} = 1.5$ nm when the field was applied along the [100] axis. In both field directions, with increasing d_{AlAs}

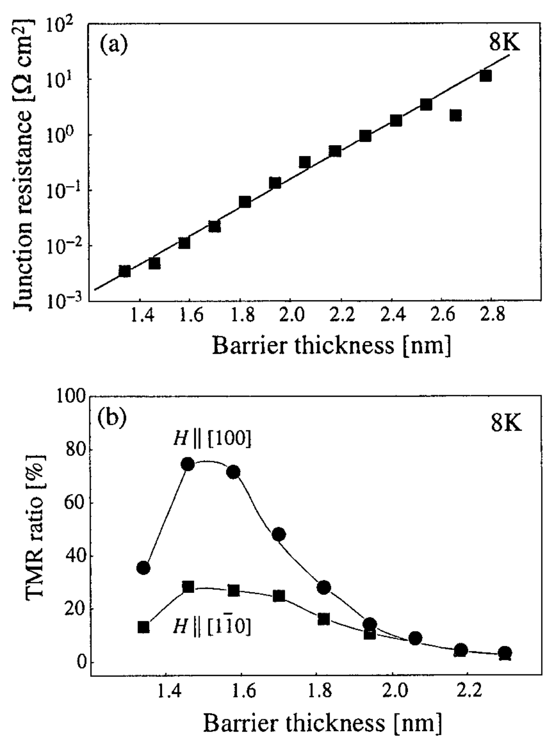

Fig. 2. Barrier thickness dependence of (a) the tunnel resistance and (b) the TMR in $Ga_{1-x}Mn_xAs$(x=4.0%, 50 nm)/ AlAs(d_{AlAs})/ $Ga_{1-x}Mn_xAs$ (x = 3.3%, 50 nm) tunnel junctions measured at 8 K. In (b), the TMR values were measured with the magnetic field applied along the [100] and [$1\bar{1}0$] axes.

(> 1.5 nm), the TMR was found to rapidly decrease from the maximum values at $d_{\mathrm{AlAs}} = 1.5$ nm. At all the values of d_{AlAs}, the TMR was higher when the field was applied along the [100] axis than along the [1$\bar{1}$0] axis. The difference of the TMR between the two directions of the field is due to the cubic magneto-crystalline anisotropy induced by the zincblende-type $\mathrm{Ga}_{1-x}\mathrm{Mn}_x\mathrm{As}$ crystal structure, where the easy magnetization axis of $\mathrm{Ga}_{1-x}\mathrm{Mn}_x\mathrm{As}$ is $\{100\}$, the detail of which is reported elsewhere.[14] Although the reason for the drop in the TMR for the junction with $d_{\mathrm{AlAs}} < 1.4$ nm is not clear at present, this drop could be caused by the decrease of the effective barrier height because of interface roughness or the image potential. Another possible reason is the ferromagnetic interlayer exchange coupling between GaMnAs layers separated by a thin AlAs layer.[11]

In Julliere's model,[15] the TMR depends only on the spin-dependent density of states in the two FM electrodes and does not depend on the barrier thickness d, so that the Julliere model cannot explain our experimental results. Because the present $\mathrm{Ga}_{1-x}\mathrm{Mn}_x\mathrm{As}$/ AlAs/ $\mathrm{Ga}_{1-x}\mathrm{Mn}_x\mathrm{As}$ heterostructures are epitaxially-grown single crystals, the wavevector $\boldsymbol{k}_{//}$ of carriers parallel to the interface should be conserved in tunneling. Calculations using the tight-binding theory including $\boldsymbol{k}_{//}$ conservation by Mathon[16] seems consistent with our experimental results of the barrier thickness dependence of the TMR.

Our experimental results can be qualitatively explained as follows: Fig. 3 shows the Fermi surfaces for up and down spins in two FM electrodes, calculated by the single-orbital tight-binding model, when the two magnetizations are (a) parallel and (b) antiparallel. Also, the dispersion of the decaying factor κ_{z} in the barrier layer was calculated and shown in the middle of the figure. The wavevector $k_{\mathrm{z}}(E_{\mathrm{F}}, \boldsymbol{k}_{//})$ normal to the interface in the FM electrodes is determined from $E_{\mathrm{F}} = E_0 + 2t\cos(k_{\mathrm{z}}a) + w(\boldsymbol{k}_{//})$, and the decaying factor $\kappa_{\mathrm{z}}(E_{\mathrm{F}}, \boldsymbol{k}_{//})$ in the barrier layer is determined from $E_{\mathrm{F}} = E_0 + 2t\cosh(\kappa_{\mathrm{z}}a) + w(\boldsymbol{k}_{//})$, where $w(\boldsymbol{k}_{//}) = 2t[\cos(k_{\mathrm{x}}a) + \cos(k_{\mathrm{y}}a)]$, $\boldsymbol{k}_{//} = (k_{\mathrm{x}}, k_{\mathrm{y}})$ is the wavevector parallel to the film plane, E_{F} is the Fermi energy, E_0 is the on-site energy in each layer, t is the nearest-neighbor hopping parameter, and a is the lattice constant.[16] We simply regard spin-polarization in the FM electrodes as the difference of E_0 between the majority and minority carriers. When the magnetizations of the two FM electrodes are parallel as shown in Fig. 3 (a), the majority (minority) spin is the up (down) spin in the both electrodes, so that the carriers can tunnel through all the channels ($\boldsymbol{k}_{//}$, σ). When the magnetizations of the two FM electrodes are antiparallel as shown in Fig. 3 (b), the up (down) spin is the majority spin in the left (right) electrode, thus the carriers with $k_{//} = |\boldsymbol{k}_{//}| > k_{\text{cut-off}}$ cannot tunnel, where $k_{\text{cut-off}}$ is the cut-off wavevector which is the largest $k_{//}$ in the minority spin band. This difference of tunneling between the parallel and antiparallel configurations indicates that the TMR is mainly caused by the carriers with large $k_{//}$ ($> k_{\text{cut-off}}$). On the other hand, the carriers with larger $k_{//}$ exponentially decay more rapidly during tunneling in the barrier because of larger κ_{z}, as shown in the middle of Fig. 3. From this in-plane dispersion of $\kappa_{\mathrm{z}}(\boldsymbol{k}_{//})$, when the barrier thickness d is large, the tunneling conductance is dominated by the carriers with smaller $k_{//}$, which do not much contribute to the TMR. Therefore, the TMR decreases as d increases.

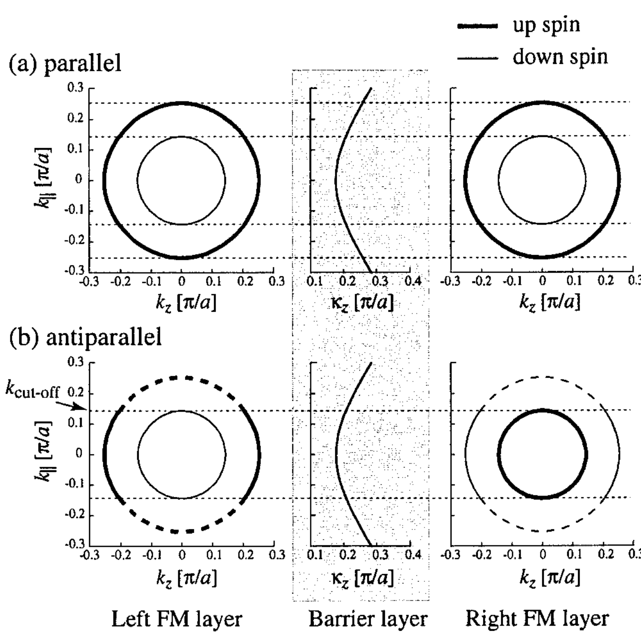

Fig. 3. Fermi surfaces of the simple cubic lattice for up and down spins with the spontaneous spin-splitting in (a) parallel and (b) antiparallel configurations. Dependence of the decaying factor κ_z in the barrier on $\boldsymbol{k}_{//}$ is also shown in the middle of the figure.

In order to compare with our experimental TMR obtained in the $\mathrm{Ga}_{1-x}\mathrm{Mn}_x\mathrm{As}$/ AlAs/ $\mathrm{Ga}_{1-x}\mathrm{Mn}_x\mathrm{As}$ tunnel junctions, we calculated the dependence of TMR on d_{AlAs} in the spin-orbit nearest-neighbor sp^3s^* model.[17,18] We used tight-binding parameters in Ref. 19 to obtain the realistic band structures of GaAs and AlAs. The effect of Mn ions in GaMnAs was simplified by introducing an additional term ΔJ_x into the intralayer coupling matrices in the sp^3s^* Hamiltonian. Here J_x is a 10×10 matrix derived from the x component of the total angular momentum $\boldsymbol{J}$ in the planar-orbital basis. We used J_x because the magnetization was along the [100] axis. This additional term causes the changes of the on-site energies proportional to J_x. The scalar proportional coefficient Δ corresponds to the spin-splitting energy between the two holes $|3/2, 1/2>$, and $|3/2, -1/2>$ at the Γ point.

Figure 4 shows the calculated (solid curve) and measured (solid circles) barrier thickness dependences of the TMR in the present $\mathrm{Ga}_{1-x}\mathrm{Mn}_x\mathrm{As}$/ AlAs/ $\mathrm{Ga}_{1-x}\mathrm{Mn}_x\mathrm{As}$ tunnel junctions. We assumed that E_{F}, V, and Δ are 0.2 eV, 0.67 eV, and 0.08 eV, respectively. E_{F} and V were measured from the top of the valence band in the calculated GaMnAs band structure, as shown in the inset of Fig. 4. $V = 0.67$ eV gives the valence band offset of 0.55 eV when $\Delta = 0$, that is, the case for normal GaAs/AlAs interfaces, which is a reasonable value. Compared with the experimental results, the calculated TMR decreases rapidly in the thinner barrier region. The barrier thickness was evaluated from RHEED oscillations and the moving speed of the shutter, as mentioned before. Because completely accurate alignment of the moving shutter with the substrate is difficult in our MBE chamber, the absolute values of the evaluated barrier thickness may not be reliable (though the relative values are reliable), thus we horizontally shifted the calculated dependence towards right (by 0.7 nm) to fit to the experimental results, as shown by

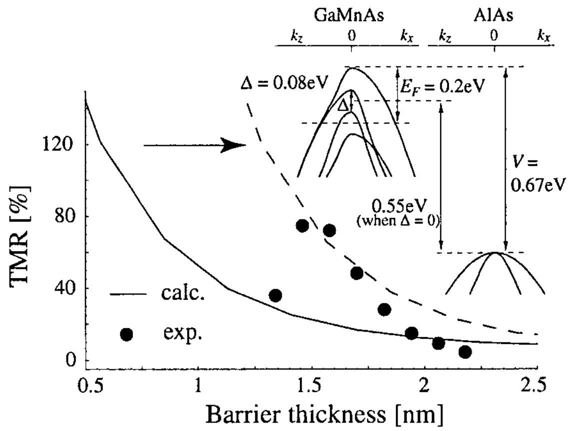

Fig. 4. Solid curve represents the calculated dependence of TMR on the barrier thickness when the Fermi energy $E_F = 0.2$ eV, the barrier height $V = 0.67$ eV (both measured from the top of the valence band of GaMnAs), and the spin splitting $\Delta = 0.08$ eV between the two light holes $|3/2, 1/2>$, and $|3/2, -1/2>$ at the Γ point. Inset shows the band dispersion and the relationship of these parameters. The solid curve is horizontally shifted by 0.7 nm to the dashed curve to fit to the experimental results (solid circles, the magnetic field was along the [100] axis), because the absolute barrier thicknesses of the junctions are nominal (see the text).

a dashed curve in Fig. 4. The fitting is fairly good but not perfect partly because the band structure of $Ga_{1-x}Mn_xAs$ is still unknown and the model is simple compared with the more complex band structure and/or partly because there could be spin scattering at the interfaces or in the tunnel barrier which is not taken into account. However, the present spin-orbit nearest-neighbor sp^3s^* model is found to explain the most essential part of the experimental barrier thickness dependence of the TMR. Note that there are three essential assumptions in this model: (1) The cut-off wavevector $k_{\text{cut-off}}$ in the plane exists in the antiparallel configuration. (2) The decaying factor κ_z in the barrier increases with increasing $k_{//}$. (3) $\boldsymbol{k}_{//}$ is conserved in tunneling. Although these assumptions may not be valid in the conventional MTJs with polycrystalline metallic electrodes, we think that they are valid in the present $Ga_{1-x}Mn_xAs$/ AlAs/ $Ga_{1-x}Mn_xAs$ tunnel junctions, which are epitaxially grown single-crystals.

In summary, we have grown $Ga_{1-x}Mn_xAs(x = 4.0\%, 50\,\text{nm})$/ $AlAs(d_{AlAs})$/ $Ga_{1-x}Mn_xAs(x = 3.3\%, 50\,\text{nm})$ single-barrier tunnel junctions by LT-MBE. In junctions with $d_{AlAs} \leqq 1.6$ nm, the TMR more than 70% (the highest value was 75%) was obtained when the field was applied along the [100] axis in the plane. The TMR rapidly decreased as the barrier thickness d_{AlAs} increased for the junctions with $d_{AlAs} > 1.5$ nm. This peculiar dependence of the TMR on d_{AlAs} was explained by calculations assuming that the parallel wavevector of carriers is conserved in tunneling.

The authors thank Dr. T. Hayashi for his contribution this work at the initial stage, and Prof. T. Nishinaga and Prof. S. Naritsuka for their support and encouragement. This work was partially supported by the JSPS Research for the Future Program (JSPS-RFTF 97P00202), the CREST Project of JST, and a Grant-in-Aid for Scientific Research from Monbusho.

References

1) T. Miyazaki and N. Tezuka: J. Magn. Magn. Mater. **139**, L231 (1995).
2) J. S. Moodera, L. R. Kinder, T. M. Wong, and R. Meservey: Phys. Rev. Lett. **74**, 3273 (1995).
3) J. S. Moodera and G. Mathon: J. Magn. Magn. Mater. **200**, 248 (1999).
4) K. Inomata: J. Magn. Soc. Jpn. **23**, 1826 (1999).
5) T. Hayashi, M. Tanaka, K. Seto, T. Nishinaga, and K. Ando: Appl. Phys. Lett. **71**, 1825 (1997).
6) M. Tanaka: J. Vac. Sci. Technol. B **16**, 2267 (1998); M. Tanaka: J. Vac. Sci. Technol. A **18**, 1247 (2000).
7) H. Ohno: J. Magn. Magn. Mater. **200**, 110 (1999).
8) Y. Ohno, D. K. Young, B. Benschoten, F. Matsukura, H. Ohno, and D. D. Awschalom: Nature **402**, 790 (1999).
9) T. Hayashi, M. Tanaka, and A. Asamitsu: J. Appl. Phys. **87**, 4673 (2000).
10) T. Hayashi, H. Shimada, H. Shimizu, and M. Tanaka: J. Crtyst. Growth **201/202**, 689 (1999).
11) D. Chiba, N. Akiba, F. Matsukura, Y. Ohno, and H. Ohno: Appl. Phys. Lett. **77**, 1873 (2000).
12) H. Shimizu, T. Hayashi, T. Nishinaga, and M. Tanaka: Appl. Phys. Lett. **74**, 398 (1999).
13) The valence band offset between GaMnAs and AlAs is unknown but it is considered to be similar to that (~0.55 eV) of GaAs and AlAs, and the Fermi energy of holes in GaMnAs is 0.1–0.2 eV, thus the barrier height V_b is ~0.45 eV. Therefore the effective mass m^* of holes which are responsible for tunneling is roughly estimated to be $\sim 0.7m_0$.
14) Y. Higo, H. Shimizu, and M. Tanaka: J. Appl. Phys., to be published.
15) M. Julli'ere: Phys. Lett. **54** A, 225 (1975).
16) J. Mathon: Phys. Rev. B **56**, 11810 (1997).
17) P. Vogl, H. P. Hjalmarson, and J. D. Dow: J. Phys. Chem. Solids **44**, 365 (1983).
18) D. J. Chadi: Phys. Rev. B **16**, 790 (1977).
19) J. N. Schulman and Yia-Chung Chang: Phys. Rev. B **31**, 2056 (1985).